Pacific and Atlantic Ocean influences on multidecadal drought frequency in the United States

Gregory J. McCabe*†, Michael A. Palecki‡, and Julio L. Betancourt§

*U.S. Geological Survey, Denver Federal Center, MS 412, Denver, CO 80225; ‡Midwestern Regional Climate Center, Illinois State Water Survey, 2204 Griffith Drive, Champaign, IL 61820; and §U.S. Geological Survey, Desert Laboratory, 1675 West Anklam Road, Tucson, AZ 85745

Edited by Inez Y. Fung, University of California, Berkeley, CA, and approved January 12, 2004 (received for review October 17, 2003)

More than half (52%) of the spatial and temporal variance in multidecadal drought frequency over the conterminous United States is attributable to the Pacific Decadal Oscillation (PDO) and the Atlantic Multidecadal Oscillation (AMO). An additional 22% of the variance in drought frequency is related to a complex spatial pattern of positive and negative trends in drought occurrence possibly related to increasing Northern Hemisphere temperatures or some other unidirectional climate trend. Recent droughts with broad impacts over the conterminous U.S. (1996, 1999–2002) were associated with North Atlantic warming (positive AMO) and northeastern and tropical Pacific cooling (negative PDO). Much of the long-term predictability of drought frequency may reside in the multidecadal behavior of the North Atlantic Ocean. Should the current positive AMO (warm North Atlantic) conditions persist into the upcoming decade, we suggest two possible drought scenarios that resemble the continental-scale patterns of the 1930s (positive PDO) and 1950s (negative PDO) drought.

Although long considered implausible, there is growing promise for probabilistic climatic forecasts one or two decades into the future based on quasiperiodic variations in sea surface temperatures (SSTs), salinities, and dynamic ocean topographies. Such long-term forecasts could help water managers plan for persistent drought across the conterminous United States (1). The urgency for such planning became evident when much of the U.S. was gripped by drought in 1996 and again in 1999–2003, evoking images of the dry 1930s and 1950s.

Analyses and forecasting of U.S. precipitation have focused primarily on the Pacific Ocean, and more specifically on oceanic indices such as those used to track the El Niño Southern Oscillation (ENSO) and the Pacific Decadal Oscillation (PDO). Much of the long-term predictability in North American climate, however, may actually reside in both observed and modeled multidecadal (50–80 years) variations in North Atlantic SSTs (2–7). Modeling studies indicate that multidecadal variability in North Atlantic climate is dominated by a single mode of SST variability (7). An important characteristic of this mode of SST variability is that the SST anomalies have the same sign across the entire North Atlantic Ocean and resemble the Atlantic Multidecadal Oscillation (AMO). The AMO is an index of detrended SST anomalies averaged over the North Atlantic from 0–70°N and has been identified as an important mode of climate variability (8). Warm phases occurred during 1860–1880 and 1930–1960, and cold phases occurred during 1905–1925 and 1970–1990. Since 1995, the AMO has been positive, but it is uncertain whether this condition will persist long enough to be considered a new warm phase. These large swings in North Atlantic SST's are probably caused by natural internal variations in the strength of ocean thermohaline circulation and the associated meridional heat transport (6, 7).

Recent analysis has shown that the AMO has a strong influence on summer rainfall over the conterminous U.S., and may modulate the strength of the teleconnection between the El Niño Southern Oscillation (ENSO) and winter precipitation (8). Positive AMO conditions (warm North Atlantic SSTs) since 1995, and the cold PDO episode from 1998 to 2002, have together raised concerns among scientists about the potential for an emerging megadrought that could pose serious problems for water planners. Here, we decompose drought frequency in the conterminous U.S. into its primary modes of variability without *a priori* consideration of climate forcing factors. These modes are then related both spatially and temporally to the PDO and AMO to determine the relative influence of the SST patterns tracked by these indices on the probability of drought. Consideration of the potential role of the Northern Hemisphere (NH) temperature or some other unidirectional trend also proved necessary to understand the variance in drought frequency. Given the time scales and current conditions of the three climate indices, we explore two possible drought scenarios for the upcoming decade.

Materials and Methods

Drought frequency for 20-year moving periods was calculated for each of the 344 climate divisions in the conterminous U.S. for the period 1900–1999. This period of record was chosen for analysis because it is common to all of the data sets used in this study (i.e., climate division precipitation, annual PDO, annual AMO, and annual NH temperature).

The climate division precipitation data were obtained from the National Climatic Data Center in Asheville, North Carolina via the internet at (http://www1.ncdc.noaa.gov/pub/data/cirs). The climate division data represent monthly means of climate station observations from regions within states that are considered to be climatically homogeneous (9). In addition, the data for the climate divisions have been corrected for time-of-observation bias (10). Although extreme climatic variations can occur in areas of complex terrain, such as the mountainous areas of the western U.S., standardized departures of temperature and precipitation from normal are spatially consistent within a climate division (9).

The PDO data were obtained from the University of Washington at (ftp://ftp.atmos.washington.edu/mantua/pnw_impacts/INDICES/PDO.latest), and the AMO data were obtained by personal communication with David Enfield (National Oceanographic and Atmospheric Administration Atlantic Oceanographic and Meteorological Laboratory, Miami). Mean annual NH temperature data also were used for part of the study and these data were obtained from the Climate Research Unit, East Anglia, U.K. (www.cru.uea.ac.uk/cru/data/temperature).

Drought conditions were considered to exist in a climate division if annual precipitation was in the lowest quartile (25%) of the 100-year record. Other definitions of drought frequency also were examined, such as the number of years with precipitation in the lowest 33% or the lowest 20% of the distribution, or annual Palmer Drought Severity Index (PDSI) values below specified thresholds; all approaches produced similar temporal and spatial results. For 20-year moving windows, the number of

This paper was submitted directly (Track II) to the PNAS office.

Abbreviations: SST, sea surface temperature; PDO, Pacific Decadal Oscillation; AMO, Atlantic Multidecadal Oscillation; NH, Northern Hemisphere.

†To whom correspondence should be addressed. E-mail: gmccabe@usgs.gov.

© 2004 by The National Academy of Sciences of the USA

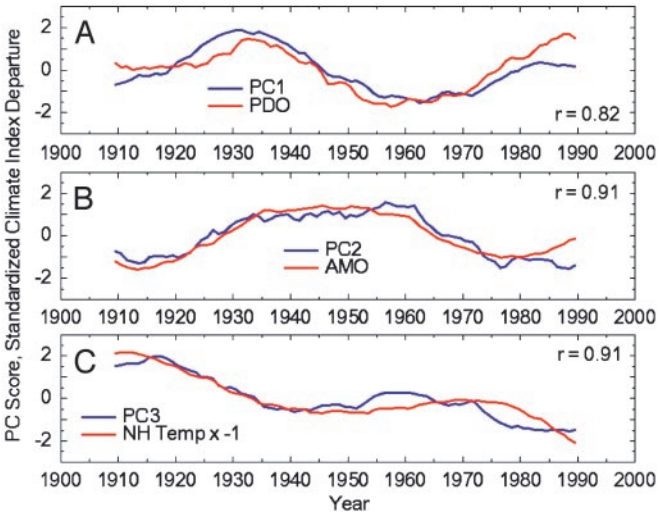

Fig. 1. Scores from the first three components (PC1, PC2, and PC3) of a rotated principal components analysis of 20-year moving drought frequency in the conterminous United States, compared to standardized departures of 20-year moving averages of the annual PDO, AMO, and NH temperature (NH Temp). The NH Temp values are multiplied by −1 for easy comparison with PC3 scores. All values are plotted at the centers of the window periods.

years with drought conditions was computed for each climate division and assigned to the center of the window period (10- and 30-year moving windows also were examined and produced results similar to those from the analysis of 20-year moving windows). The time series of 20-year moving drought frequencies (hereafter referred to as drought frequency) then were subjected to a rotated principal components analysis (RPCA) with varimax rotation to identify the primary modes of variability in the drought frequency data. The scores and loadings of the leading rotated principal components were subsequently examined and compared with 20-year moving averages of the PDO and AMO to better understand how these climate indices are related to the temporal and spatial variability of drought in the conterminous U.S.

Results and Discussion

The rotated principal components analysis (RPCA) of drought frequencies for the 344 climate divisions in the conterminous U.S. produced three leading components (PC1, PC2, and PC3) that explain 74% of the total variance in the drought frequency data; after varimax rotation, PC1 explains 24% of the total variance in drought frequency, PC2 explains 28%, and PC3 explains 22%. The score time series (Fig. 1) illustrate the temporal variability of the drought frequency components, and the loadings (Fig. 2 *A–C*) illustrate the spatial pattern of drought frequency variability represented by each component.

The scores for PC1 (Fig. 1*A*) are positive for 20-year periods centered from around 1920 to the mid- to late 1940s, are negative from the late 1940s until the late 1970s, and are slightly positive after the 1970s. This decadal variability in drought frequency is similar to variability in the PDO (Fig. 1*A*). The correlation between PC1 scores and 20-year moving mean annual PDO is 0.82.

Because of the large autocorrelation inherent in smoothed time series, the degrees of freedom must be estimated to use standard statistical significance tests. Instead, an alternative approach was used to assess the significance of the correlations between the PC score and climate index time series. A Monte Carlo approach (11) was used that involves the shuffling of the raw climate index time series 1,000 times. Each shuffled time series was subsequently smoothed with a 20-year moving average and then correlations between the smoothed shuffled time series and the PC scores were computed. The 95th and 99th percentiles of the resulting correlations (0.69 and 0.83, respectively) then were compared with the correlations obtained between the PC scores and the observed 20-year moving average climate index time series. The results of this analysis indicated that the correlation ($r = 0.82$) between the time series shown in Fig. 1*A* is between the 98th and 99th percentile of correlations from the 1,000 trials, indicating a high level of statistical significance.

To further compare PC1 with PDO, the loadings of drought frequency for each climate division on PC1 (Fig. 2*A*) were compared with correlations between 20-year moving average annual PDO and drought frequency for each climate division (Fig. 2*D*). Comparison of these figures indicates that the patterns of the PC1 loadings and the PDO correlations are similar. Both indicate negative values for the southwestern U.S. that extend into the Rocky Mountain region and the south-central U.S. (Fig. 2 *A* and *D*). Negative values also are found in the northeastern U.S. Positive values are indicated in the northwestern U.S., the north-central plains, and most of the southeastern U.S. The correlation between these patterns is 0.92. The PDO has been shown previously to modulate winter precipitation in the U.S. (12–14), as well as summer drought and streamflow in the conterminous U.S. (15).

The strong correlation of the spatial patterns represented by the PC1 loadings and the PDO correlations (Fig. 2 *A* and *D*), when combined with the magnitude of the time series correlation, strongly supports the conclusion that the first mode of drought frequency identified in this study is a response to the multidecadal variability of the PDO. The annual response pattern is a combination of the winter and summer influences of PDO on precipitation. Although both seasons share a dipolar response in the northwest and southwest U.S., the response to the PDO in the Midwest is of a different sign in the summer and winter, weakening the annual response in that region.

The scores for PC2 increase from the early part of the record to the 20-year period centered around 1930. The score values remain relatively constant until after 1960, when they decline until the end of the period of record (Fig. 1*B*). This time series corresponds to the temporal variability of the AMO (Fig. 1*B*). The correlation between PC2 scores and 20-year moving average annual AMO is 0.91, which is significant at the 99th percentile.

Loadings for PC2 (Fig. 2*B*) and correlations between 20-year moving average annual AMO and drought frequency (Fig. 2*E*) are highly similar (the correlation between these patterns is 0.95). Maps of the PC2 loadings and the AMO correlations indicate positive values for most of the central two-thirds of the conterminous U.S. and suggest an almost nationwide covariance of drought frequency (Fig. 2 *B* and *E*). Previous research has shown that, during positive AMO conditions, the central U.S. receives below-average precipitation, particularly during summer (1, 8). The large positive correlations between smoothed AMO and drought frequency for the central U.S. (Fig. 2*E*) support this statement. This mode explains 28% of the variance in drought frequency, and covers a large geographical area with uniformly strong loadings. Correlations between smoothed AMO and similarly smoothed climate division precipitation (the inverse of drought frequency) produced a continental-scale pattern of negative correlations (8).

Scores for PC3 indicate a long-term negative trend (Fig. 1*C*). Areas with negative loadings had an increasing trend in drought frequency (Fig. 2*C*), whereas areas with positive loadings had a decreasing trend in drought frequency. Geographically, California, the northern Rocky Mountains, and the Ohio Valley (negative loadings) have experienced an increasing tendency for drought, whereas the Pacific Northwest, a band from New York

ECOLOGY

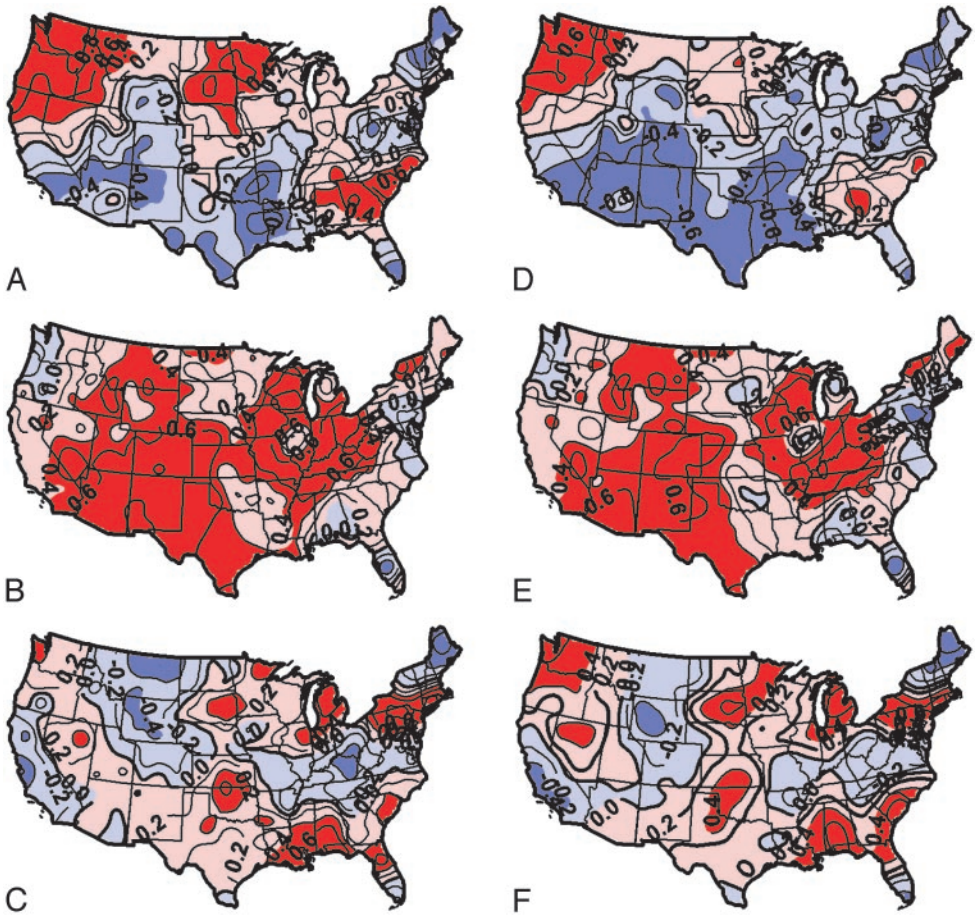

Fig. 2. (*A–C*) Loadings for the first three components of a rotated principal components analysis of 20-year moving drought frequency in the conterminous United States. (*D*) Correlations between 20-year moving drought frequencies and 20-year moving annual PDO. (*E*) Correlations between 20-year drought frequency and 20-year moving AMO. (*F*) Inverse of trends in 20-year drought frequency. The correlations in *F* were multiplied by −1 for easy comparison with other figures. Positive values are shaded red, and negative values are shaded blue. Darker shades indicate values >0.4 or <−0.4.

to the Upper Midwest, and the Gulf Coast (positive loadings) have had a decreasing tendency for drought.

The pattern of loadings for PC3 (Fig. 2*C*) is very similar to the spatial pattern of the inverse of trends in 20-year moving drought frequency (Fig. 2*F*) (correlation coefficient is 0.91). The trends in 20-year moving drought frequency were multiplied by −1 for direct comparison with the PC3 loadings and were computed as linear correlations with time.

The PC3 score time series does not appear to be related to known atmosphere–ocean modes of variability; instead, it matches well with both a trend line and the time series of mean annual NH temperature. In Fig. 1*C*, the NH temperatures were multiplied by −1 for direct visual comparison with the scores for PC3. Instrumental observations of NH temperatures indicate a generally increasing trend with some distinct inflections over the period of record used in this study (16); the inverse 20-year moving mean annual NH temperatures are significantly correlated with PC3 scores (correlation coefficient is 0.91, $P < 0.01$).

These results suggest that PC3 reflects a regional pattern of changes within the hydrologic cycle that may be related indirectly with increases in NH temperature, or may be trending in response to some other forcing that has not yet been identified. Climate modeling studies indicate that a substantial intensification of the global hydrologic cycle is likely in a warming world, although the regional patterns of temperature and precipitation responses are likely to be complex (16).

Because previous research showed relations between drought in the conterminous U.S. and El Niño/Southern Oscillation (ENSO) (17), we compared 20-year moving averages of annual NINO3.4 SSTs, representing ENSO conditions, with the PC scores of drought frequency examined in this study (NINO3.4 SSTs are averaged for the region from 5°N latitude to 5°S latitude and from 170°W longitude to 120°W longitude; these data were obtained via the internet from http://climexp.knmi.nl).

Correlations between the smoothed NINO3.4 time series and the PC scores were strongest for PC2 (−0.58). This correlation with PC2 scores is much weaker than the correlation between PC2 scores and the similarly smoothed AMO (0.91), and is not statistically significant.

To test the interpretation of the PCA analysis that PDO, AMO, and a trend such as that represented by NH temperature explain a large percent of the temporal and spatial variability in multidecadal drought frequency in the conterminous U.S., regressions were developed to estimate drought frequency for the 344 climate divisions of the conterminous U.S. The regressions were developed by using 20-year moving drought frequency as the dependent variable and 20-year moving average annual PDO, AMO, and NH temperature as the independent variables. The median coefficient of determination for the regressions for all 344 climate divisions was 0.72 (the mean was 0.68, the first quartile was 0.58, and the third quartile was 0.81), indicating that, on average, ≈70% of the temporal variability in drought fre-

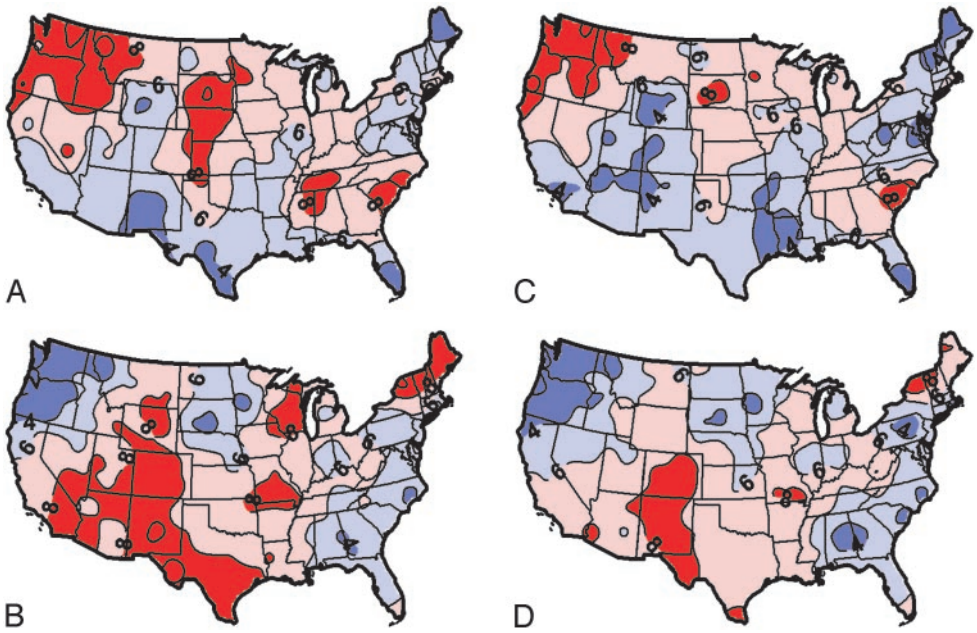

Fig. 3. Observed (*A* and *B*) and simulated (*C* and *D*) 20-year drought frequency (in years) for 1924–1943 (the 1930s drought) and 1947–1966 (the 1950s and 1960s droughts). Areas with drought frequencies of 6 years or more are indicated in red.

quency for the climate divisions is explained by the PDO, AMO, and NH temperature.

The reliability of the regressions to explain the spatial variability in drought frequency was evaluated by comparing observed and simulated drought frequency for specific periods (Fig. 3). Because 20-year moving periods were used to compute drought frequency, the period for 1924–1943 provided an example incorporating the 1930s drought, and the period 1947–1966 was chosen to encompass both the 1950s drought and the 1960s Northeast drought. Results indicate that the spatial distributions of drought frequency for these periods represented by the observed and simulated drought frequencies are highly similar. The correlation between the observed and simulated drought frequency values for the 1924–1943 period (Fig. 3 *A* and *C*) is 0.91 ($P < 0.01$), and for the 1947–1966 period (Fig. 3 *B* and *D*), the correlation is 0.92 ($P < 0.01$). The correlations between observed and simulated drought patterns for all 20-year periods examined in this study ranged from 0.70 to 0.95, with a median value of 0.88.

To validate the robustness of the regressions used to simulate the spatial patterns of drought for the 1924–1943 and the 1947–1966 periods, additional regressions were developed, excluding in each case the 20-year periods of interest. The correlations between the observed and simulated spatial patterns of drought using the new regressions were 0.83 ($P < 0.01$) for 1924–1943 and 0.86 ($P < 0.01$) for 1947–1966. These correlations, although somewhat smaller than those using all of the data, indicate that the regressions are robust.

These results indicate that, in addition to reliably explaining the temporal variability in drought frequency, the regression equations also reliably explain the spatial variability in drought frequency. Without inclusion of all three time series, the PDO, AMO, and NH temperature, the fidelity of the regression modeled drought frequency pattern with the observed pattern is substantially reduced.

So what are the prospects for drought under varying PDO and AMO regimes? Annual time series of PDO and AMO were used to identify periods of positive and negative PDO and AMO regimes (Fig. 4). Four periods were identified: (*i*) positive PDO and positive AMO (1926–1943), (*ii*) negative PDO and positive AMO (1944–1963), (*iii*) negative PDO and negative AMO (1964–1976), and (*iv*) positive PDO and negative AMO (1977–1994). Composite drought frequencies were computed for the four combinations of PDO and AMO regimes. The drought frequencies were determined by counting the number of years at each climate division with annual precipitation in the lowest quartile of the 1900–1999 record, and were expressed as a percent of the total number of years in each PDO/AMO regime category. Because the normal rate of occurrence of precipitation in the lowest quartile is 25% of the time, composite percentages >25% represent a greater than normal probability of drought, and values <25% characterize less than normal chances of drought.

Fig. 5 shows drought frequencies for the four general scenarios based on different combinations of the AMO and PDO. In the case of negative AMO, above normal drought frequency is restricted to a few regions, for example, to the Pacific Northwest and Maine during positive PDO (Fig. 5*A*) and southern California and the central High Plains during negative PDO (Fig. 5*B*). Irrespective of the PDO phase, positive AMO is associated with an above normal frequency of drought across large parts of the U.S. With positive AMO and positive PDO (Fig. 5*C*), the pattern is more reminiscent of the 1930s drought, sparing the Southwest but entraining the northern two-thirds of the U.S. With positive AMO and negative PDO (Fig. 5*D*), the pattern is that of the 1950s drought with the greatest impact in the Midwest, Southwest, and the Rocky Mountains/Great Basin area.

Because the AMO generally has greater multidecadal persistence than the PDO, North Atlantic warming that began in 1995 may continue. After a negative downturn in mid-1998, the PDO reversed sign in mid-2002. Given the current positive anomalies in North Atlantic SSTs (positive AMO), continuation of the present 1999–2003 drought is more likely than normal, and a decadal-scale drought may be emergent. The pattern of recent drought in the conterminous U.S. resembles a 1950s-like drought (positive AMO and negative PDO) (Figs. 3*B* and 5*D*). However, if the AMO continues to be positive and the PDO becomes

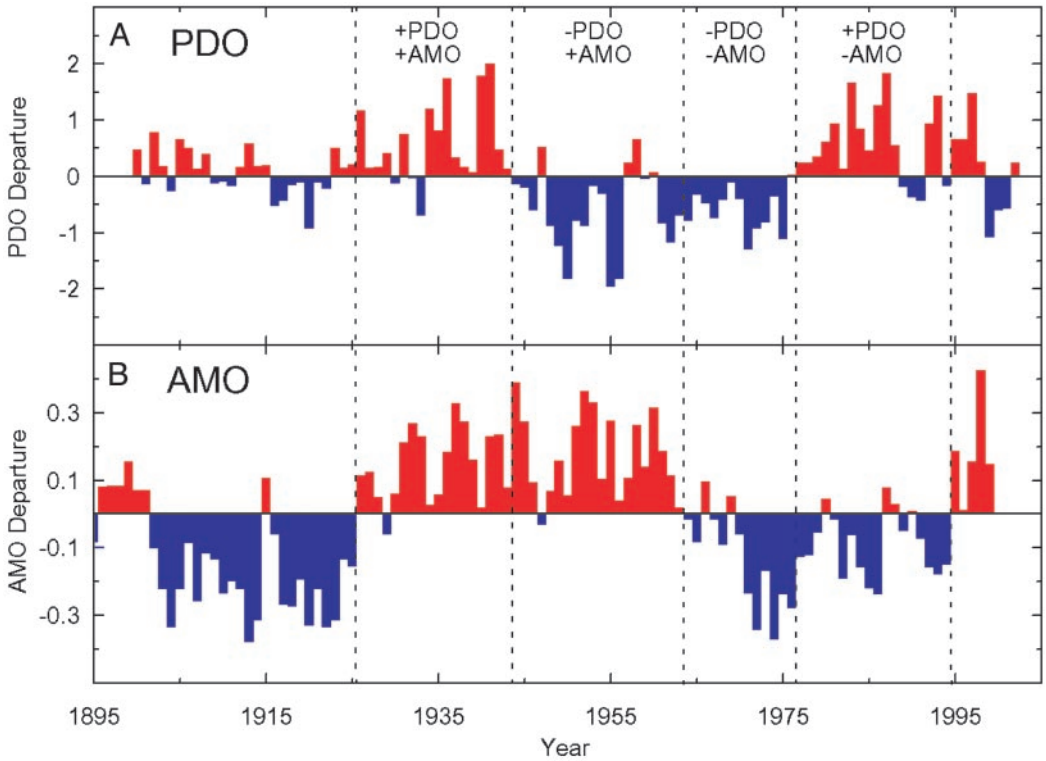

Fig. 4. Time series of the annual PDO and AMO. Shaded areas indicate combinations of positive (+) and negative (−) PDO and AMO periods.

positive, the drought pattern could shift to one more like the 1930s era (Figs. 3*A* and 5*C*). Although it is always prudent to be conservative about water resources, particularly in the semiarid West, it may be particularly necessary in the next decade.

Conclusions

Three rotated principal components explain 74% of the variance in 20-year moving frequencies of drought in the conterminous U.S. The first component is highly correlated with the PDO, and the second component is correlated with the AMO. These first two components explain nearly equal proportions of variance in the entire data set and, combined, explain 52% of the total variance. These results support previous research that has indicated the existence of a relation between these climate indices and drought variability in the U.S. The third component represents a complex pattern of positive and negative trends in U.S.

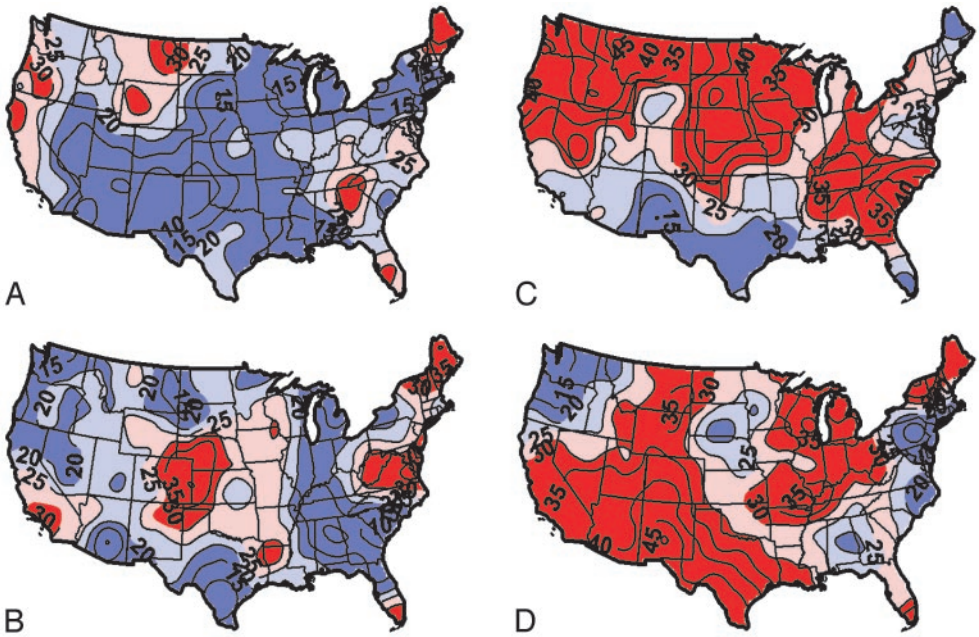

Fig. 5. Drought frequency (in percent of years) for positive and negative regimes of the PDO and AMO. (*A*) Positive PDO, negative AMO. (*B*) Negative PDO, negative AMO. (*C*) Positive PDO, positive AMO. (*D*) Negative PDO, positive AMO.

drought frequency over the 20th Century, and its score time series is highly correlated with both a trend line and the inverse NH temperature time series. The inclusion of all three time series, the PDO, AMO, and a trending geophysical indicator like NH temperature, appears to be crucial in generating multiple regression equations that can accurately simulate the historical 20-year patterns of drought frequency. This research indicates that persistence of the current positive AMO state may lead to continuing above normal frequencies of U.S. drought in the near future, with the pattern of drought modulated by the sign of the PDO.

This work was partially supported by National Oceanographic and Atmospheric Administration Cooperative Agreement NA67RJ0146.

1. Gray, S. T., Betancourt, J. L., Fastie, C. L. & Jackson, S. T. (2003) *Geophys. Res. Lett.* **30,** 10.1029/2002GL016154.
2. Folland, C. K., Palmer, T. N. & Parker, D. E. (1986) *Nature* **320,** 602–606.
3. Schlesinger, M. E. & Ramankutty, N. (1994) *Nature* **367,** 723–726.
4. Griffies, S. M. & Bryan, K. (1997) *Science* **275,** 181–184.
5. Delworth, T. L. & Mann, M. E. (2000) *Climatic Dyn.* **16,** 661–676.
6. Collins, M. & Sinha, B. (2003) *Geophys. Res. Lett.* **30,** 10.1029/2002GL016504.
7. Sutton, R. T. & Hodson, L. R. (2003) *J. Clim.* **16,** 3296–3313.
8. Enfield, D. B., Mestas-Nunez, A. M. & Trimble, P. J. (2001) *Geophys. Res. Lett.* **28,** 277–280.
9. Karl, T. R. & Riebsame, W. E. (1984) *J. Clim. Appl. Meteorol.* **23,** 950–966.
10. Karl, T. R., Williams, C. N., Young, P. J. & Wendland, W. M. (1986) *J. Clim. Appl. Meteorol.* **25,** 145–160.
11. Livezey, R. E. & Chen, W. (1983) *Mon. Weather Rev.* **111,** 46–59.
12. Mantua, N. J. & Hare, S. R. (2002) *J. Oceanogr.* **58,** 35–44.
13. Mantua, N. J., Hare, S. R., Zhang, Y., Wallace, J. M. & Francis, R. C. (1997) *Bull. Am. Meteorol. Soc.* **78,** 1069–1079.
14. McCabe, G. J. & Dettinger, M. D. (1999) *Int. J. Climatol.* **19,** 1399–1410.
15. Nigam, S. M., Barlow, M. & Berbery, E. H. (1999) *Eos (Washington, D.C.)* **80,** 621–625.
16. Houghton, J. T, Ding, Y. Griggs, D. J., Noguer, M., Van der Linden, P. J., Dai, X., Maskell, K. & Johnson, C. A., eds. (2001) *Climate Change 2001: The Scientific Basis* (Cambridge Univ. Press, Cambridge, U.K.).
17. Dai, A., Trenberth, K. E. & Karl, T. R. (1998) *Geophys. Res. Lett.* **25,** 3367–3370.